J. Biochem. 2010;148(1):103–113 doi:10.1093/jb/mvq039

JB THE JOURNAL OF BIOCHEMISTRY

Functional study on GTP hydrolysis by the GTP-binding protein from *Sulfolobus solfataricus*, a member of the HflX family

Received March 2, 2010; accepted April 2, 2010; published online April 16, 2010

Bo Huang[1], Hao Wu[2], Ning Hao[1], Fabian Blombach[3], John van der Oost[3], Xuemei Li[1], Xuejun C. Zhang[1,2,*] and Zihe Rao[1]

[1]Institute of Biophysics, Chinese Academy of Sciences, 15 Datun Road, Chaoyang District, Beijing 100101, China; [2]Protein Studies Program, Oklahoma Medical Research Foundation, 825 Northeast 13th Street, Oklahoma City, OK 73104, USA; and [3]Laboratory of Microbiology, Wageningen University, Dreijenplein 10, 6703 HB Wageningen, Netherlands

*Xuejun C. Zhang, Institute of Biophysics, Chinese Academy of Sciences, 15 Datun Road, Beijing 100101, China.
Tel: +86 10 64889186; Fax: +86 10 64888554;
email: zhangc@ibp.ac.cn

GTPase domains from members of the HflX protein family have their catalytic glutamine residue of the DxxGQ motif substituted by phenylalanine, while they are still able to hydrolyse GTP. This appears to challenge the traditional view of GTP hydrolysis mechanism of Ras-like GTPases. SsGBP from the hyperthermophilic archaeon *Sulfolobus solfataricus* provided the first crystal structure of the HflX family. Here, we report structure-based mutagenesis analyses on SsGBP. Six-point mutations were individually introduced in the Ras-like GTPase domain including regions of P-loop, switches I and II. Intrinsic GTPase activities and thermal stabilities of these variants together with the wild-type full-length SsGBP and its isolated GTPase domain were analysed. Both functional and structural analyses of G235P and G235S mutants, which showed total and partial loss of the GTP hydrolyzing activity, respectively, support our hypothesis that the role of aligning a nucleophilic water molecule by the Ras Gln60 residue is replaced by the backbone amide group of Gly235 in SsGBP. Together with functional studies of other mutants, we conclude that the classical view of GTP hydrolysis mechanism likely remains the same in the HflX family with a twist in the entity of the nucleophilic alignment.

Keywords: crystal structure/GTPase/HflX/mutation/SsGBP.

Abbreviations: EDTA, ethylenediaminetetraacetic acid; GDP, guanosine diphosphate; GTP, guanosine triphosphate; SsGBP, Sulfolobus solfataricus *GTP* binding protein; WT, wild type.

GTP-binding protein from the hyperthermophilic archaeon *Sulfolobus solfataricus* (SsGBP) is a two-domain protein with its crystal structure reported recently (*1*). Its amino (N)-terminal domain (referred as N-domain, residues 1–178) has a novel α/β/α folding and is conserved at the primary sequence level among members of the so called HflX family (*1*, *2*); therefore, this domain is designated as HflX folding. Meanwhile the carboxyl (C)-terminal domain (referred as G-domain, residues 179–356) of SsGBP is of a typical folding of classical Ras-like GTPases (also called small GTPases) and shares several conserved regions with the latter (*1*), which are essential for the GTP hydrolysis (*3*). More importantly, the GTPase activity has been demonstrated in recombinant SsGBP (*1*).

While SsGBP currently represents the only member of the HflX family whose 3D structure has been determined at high resolution, members of the HflX family are widely distributed in all three domains of life. HflX members in *Escherichia coli* and *Chlamydophila pneumoniae* are, for example, reported to interact with the 50S subunit of ribosome and to function in ribosome assembly (*4*, *5*). In addition, in *E. coli* the GTPase activity of HflX homologue can be stimulated by the 50S ribosomal subunit (*6*). Related to these observations in homologous proteins, SsGBP is also believed to bind ribosomal RNA (*1*), and such an HflX specific function is likely to be directly associated with the N-terminal HflX domain. However, the relationship between the nucleotide binding and GTPase activity of SsGBP remains to be determined.

The C-terminal GTPase domain of SsGBP is believed to be where the GTPase activity resides (*1*). Small GTPases usually function as molecular switches by cycling their conformations between a GTP-bound active form and a GDP-bound inactive form. GTP hydrolyzing mechanism and corresponding conformational changes of small GTPases are among the best studied biological processes (*3*). Regions of a small GTPase key to its enzyme activity include the P-loop, switches I and II as well as GTP-specificity recognition sites. The P-loop forms hydrogen bonds with the β–γ bridge oxygen ($O_{\beta\gamma}$) and other phosphoryl oxygen atoms of the GTP substrate. Such a binding facilitates formation of the transition state of the hydrolysis reaction (*7*). This P-loop is conserved among HflX members. The switch I region is usually the most flexible part of the enzyme in response to GTP binding and hydrolysis. This region in SsGBP is also mobile in the previously published SsGBP crystal structures. Moreover, the switch II region contains a conserved DxxGQ motif (where x stands for any amino-acid residue) in small GTPases (*e.g.* residues 57–61 in human Ras) (*3*, *8*). The conserved glutamine residue plays a crucial role in aligning a nucleophilic water molecule to interact with the γ-phosphoryl group along the axial

direction of the $O_{\beta\gamma}$–P_{γ} bond. Point mutations to hydrophobic residues at this glutamine position usually result in abolished activity for Ras-like GTPases (*9–11*). However, in the entire HflX family, all GTPases contain a hydrophobic residue at this position. In particular, a phenylalanine residue in SsGBP replaces the glutamine residue of the DxxGQ motif. It immediately raises a few questions about the GTP hydrolysis mechanism of the SsGBP G-domain: (i) Does SsGBP share the same catalytic mechanism with canonical small GTPases? (ii) What is the function of this hydrophobic residue conserved in the HflX family? And (iii) what functional group in SsGBP replaces the role of the classical glutamine in a Ras-like small GTPase?

In this study, we tried to address the above questions from several aspects. First, by analysing results from a metal dependence activity assay and a new crystal form of the wild-type (WT) SsGBP•GDP complex we demonstrated that SsGBP behaves like a classical small GTPase in terms of requirement of a magnesium ion for guanine nucleotide binding. Second, in order to compare the GTP hydrolysis mechanism of SsGBP with the classical one, we introduced six-point mutations to probe the catalytic site of SsGBP including P-loop; switches I and II and measured their intrinsic GTPase activities. Third, we performed thermostability experiments (*12*) on every mutant variants to show that the activity changes of the mutants were not due to a possibility of their reduced stability. Additionally, we solved the crystal structures of G235P and G235S and illustrated that the catalytic sites in these two mutant variants maintained a similar conformation as in the WT. Our current data suggests that (i) the conserved phenylalanine in the DxxGF sequence of the HflX family is involved in regulation of the interaction between N- and G-domain and of the GTPase activity of SsGBP; and (ii) P-loop and switch I maintain their classical functions in SsGBP, while the backbone amide group of SsGBP Gly235 most likely replaces the role of the catalytic glutamine side chain in the classical GTPases.

Results

Mg^{2+} dependency of the GTPase activity of WT SsGBP

It has been shown that Ras-like GTPases require magnesium ion (Mg^{2+}) for their full activity. However, in the previously published 2.0 Å resolution SsGBP•GDP complex crystal structure (PDB ID 2QTH), the 'active site' Mg^{2+} ion was accompanied by a cadmium ion (Cd^{2+}) at a 4.5-Å distance and appeared to be pushed away from its normal position. This observation raised questions about the role of Mg^{2+} in SsGBP GTP hydrolysis. Therefore, we first investigated whether Mg^{2+} is specifically required for the GTPase activity following the classical GTPase mechanism. Furthermore, we tested the possible effect of Cd^{2+}on GTPase activity of SsGBP. Since Cd^{2+} is unlikely to be a physiological relevant ion, we also tested Ca^{2+} which has a ionic radius similar to Cd^{2+}. The time courses of GTP hydrolysis by the recombinant WT SsGBP in the presence of three different divalent metal ions were measured (Fig. 1). The result showed that while Cd^{2+} and calcium ion (Ca^{2+}) did not enhance the activity, 5 mM additional Mg^{2+} increased the GTPase activity (*i.e.* the amount of GTP hydrolyzed during a pre-determined time interval, Fig. 1A) of WT SsGBP, and this enhanced activity could be reversed by adding 100 mM EDTA (ethylenediaminetetraacetic acid). These data indicated that similar to Ras-like GTPases, SsGBP requires Mg^{2+} for its full GTPase catalytic activity.

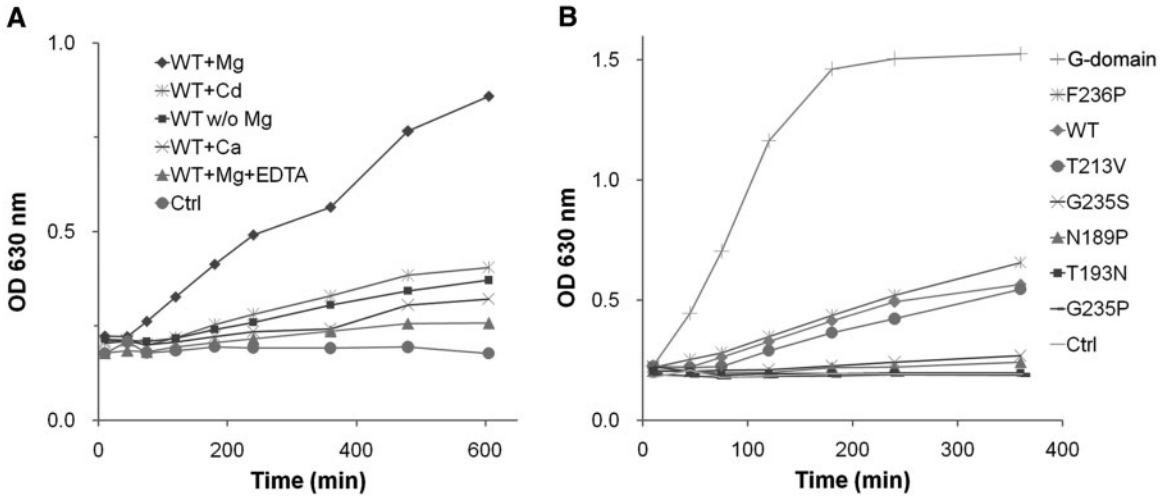

Fig. 1 Time course of GTP hydrolysis of WT SsGBP, the C-terminal GTPase domain (G-domain) and different point mutations. At each indicated time point, a 50 µl aliquot of the reaction mixture was withdrawn for measurement of phosphate release using the malachite-green assay (see 'Methods' section for detailed information about the assay). Each curve shown here is a representative of two independent experiments in which aliquots were taken at slightly different time points but the results were similar. (A) GTP (100 µM) hydrolysis by WT SsGBP (5 µM) with or without additional divalent metal ions ($MgCl_2$, $CaCl_2$ or $CdSO_4$ at 5 mM). The control reaction contained no protein sample. (B) Effects of point mutations on the GTP hydrolysis activity of SsGBP. Labels of the samples in panels A and B are ordered according to their relative GTPase activities.

Crystal structure of WT SsGBP and GDP complex

Although Mg^{2+} was shown to be required for the GTPase activity of SsGBP, it was still possible that the detailed mechanism of Mg^{2+} in SsGBP differs from that of other small GTPases. In particular, in most of the currently available complex structures of GTPases with either GDP or GTP, the Mg^{2+} ion residing in the active site is coordinated by β (and γ) phosphoryl group(s) of GDP (GTP); in contrast, the complex crystal structure of WT SsGBP•GDP in our previous paper (*1*) showed that the Mg^{2+} ion in the active site interacted with both α and β-phosphoryl groups of GDP. Thus SsGBP appeared to be an abnormal GTPase, which warranted further structural analysis of SsGBP to verify the role of its required Mg^{2+} ion.

We obtained WT SsGBP•GDP crystals under a different condition from the previously reported one (*13*) in the presence of GDP, NaF and $AlCl_3$. Our crystal form has cell parameters of a = 67.3 Å, b = 68.5 Å and c = 92.1 Å and belongs to space group $P2_12_12_1$. There is one SsGBP molecule (residues 1–356) per asymmetric unit with a 54% solvent content (Matthews coefficient $V_M = 2.7\,Å^3/Da$). The structure was solved using the molecular replacement method and refined at 2.5 Å resolution to final $R_{work} = 0.23$ and $R_{free} = 0.29$. Total 326 amino-acid residues and seven solvent molecules were included in the final refined model. However, we did not observe AlF_3 as part of a transition state analogue (*7*, *14*). Thus, this structure represents a GDP bound form of SsGBP. Hereafter, we will refer our new SsGBP•GDP complex crystal structure as WT SsGBP•GDP, while the previously published SsGBP•GDP complex crystal structure is referred by its PDB ID, 2QTH. The root mean square deviation (r.m.s.d.) between our structure and 2QTH was 1.1 Å for 309 Cα pairs (all available common Cα atoms from the two structures were included in the calculation hereafter unless otherwise specified). There was essentially no change in the relative position between the N- and G-domains. Nevertheless, we observed some localized differences between the two structures. First, in our structure the Mg^{2+} ion only contacted the β-phosphoryl group (Fig. 2). This discrepancy of Mg^{2+} position between the two SsGBP•GDP structures may be attributed to the fact that we co-crystallized SsGBP and GDP in this study while the ligand was soaked into the protein crystals which

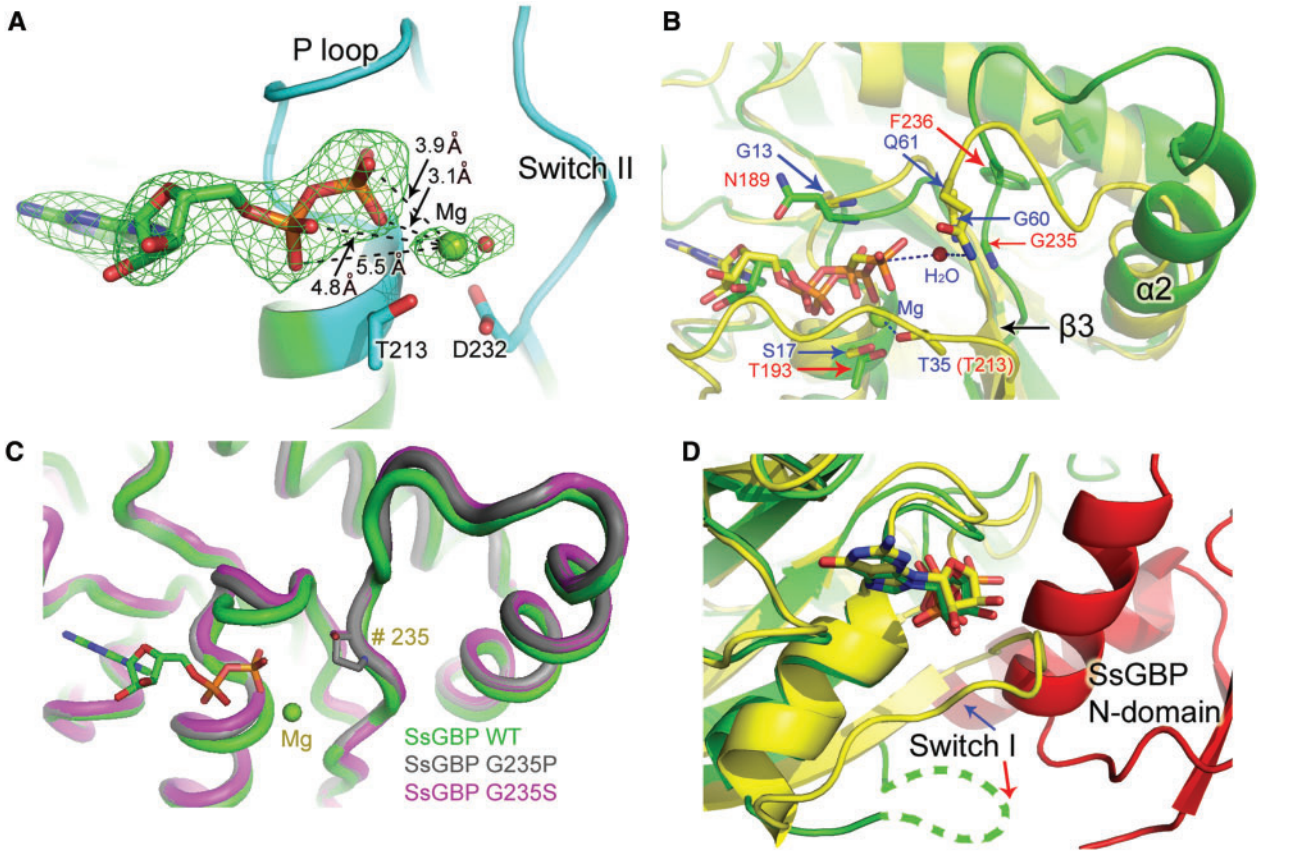

Fig. 2 Structural analysis on GTPase active site of SsGBP. (A) Binding of Mg^{2+} to GDP in the active site (cyan) of WT SsGBP. An F_{obs}–F_{calc} omit map (green) was contoured at 3.0σ. In order to calculate this map, GDP, Mg^{2+}, and the related water molecules were omitted by setting their occupancy to zero followed by a few cycles of refinement to reduce potential bias. (B) GTPase domain of WT SsGBP•GDP (green) and Ras•GppCp (PDB ID 6Q21_B) (GppCp, *i.e.* phosphomethylphosphonic acid guanylate ester is a non-hydrolyzable GTP analogous) (yellow) were superimposed on each other. The point mutation sites of SsGBP (labeled in red) and their equivalent positions in Ras (labeled in blue) are shown, except Thr213 of SsGBP which is excluded because of high mobility of the switch I region. Note that SsGBP Phe236 interacts with a hydrophobic core of G-domain. Also the hinge region connecting β3 and α2 in SsGBP is longer than that in Ras. (C) Structure comparison of WT SsGBP•GDP (green), G235P (grey) and G235S (magenta). The side chains of residue 235 are shown in *stick* models. (D) Ras•GppCp (6Q21_B) (yellow) and WT SsGBP•GDP (green) were superimposed in the presence of SsGBP N-domain (red). Switch I regions of SsGBP and Ras are pointed by red and blue arrows, respectively. The former is represented by a dash line implicating that it is mobile in the crystal structure.

were grown in the presence of Cd^{2+} ion in the previous work (*13*). Second, a mobile loop region, *i.e.* residues 168–174 in the 2QTH structure became involved in a crystal packing in our currently described one and consequently gained visible electron density sufficient for peptide tracing (Supplementary Fig. S1). On the other hand, the mobile loop regions of residues 123–141 and 204–215 in 2QTH remained flexible in the new crystal form. Among other conclusions, our new crystal structure of the WT SsGBP confirmed the classical role of Mg^{2+} in guanine nucleotide binding, which differs from the picture presented by previous SsGBP crystal structures.

Point mutation variants of SsGBP

To study the relationship between functional mechanisms of SsGBP and Ras-like small GTPases, six-point mutation variants of SsGBP, namely N189P, T193N, T213V, G235P, G235S and F236P were constructed in the full-length WT parental background, some of which were based on homologous mutations in Ras-like GTPases (*7*, *15*, *16*) (Figs 2B and Supplementary Fig. S2). In particular, the N189P mutation was located in the P-loop and mimicked a previously reported inactivate point mutation of a Ras-like GTPase, Rab5 (*7*). In Rab5, the corresponding A30P variant is one of a few mutants at this position that deactivate the GTPase, yet the crystal structure of A30P complexed with GTP was determined, illustrating that structural effects of such a mutant are localized (*7*). The T193N mutation mimicked the classical SN mutant of Ras-like GTPases, which usually inhibits GDP–GTP exchange and causes the GTPase to stay in the GDP-binding state (*16*). The T213V mutant was located in the putative switch I region of SsGBP, and in Ras the side chain of corresponding residue participates in the coordination of the catalytic Mg^{2+}. T213V would potentially maintain the same side chain geometry at position 213 but would eliminate its bonding ability towards the Mg^{2+} ion. The rest three-point mutations were located in the conserved DxxGF sequence of the HflX family which corresponds to the DxxGQ motif of Ras-like small GTPases. Among them, G235P and G235S were designed to test functions of Gly235, particularly its backbone amide group, in GTP hydrolysis. F236P was designed to probe the conserved, hydrophobic, switch II residue of the DxxGF sequence.

To determine the GTPase activity and measure kinetic data of every mutant, WT SsGBP and the isolated C-terminal GTPase domain, the malachite green assay (*17*) was conducted (Figs 1B and 3). The isolated C-terminal GTPase domain was included in this study to provide a baseline of the GTPase activity in the absence of the N-domain. Consistent with data reported previously (*1*), our recombinant WT SsGBP had a k_{cat} of $0.024 \pm 0.001\,min^{-1}$ and a K_m of $5.3 \pm 0.8\,\mu M$ (Fig. 3); and the isolated GTPase domain showed a higher activity with $k_{cat} = 0.051 \pm 0.001\,min^{-1}$ and $K_m = 4.8 \pm 0.4\,\mu M$. Among the six mutants, F236P was the only one showing enhanced k_{cat} ($0.032 \pm 0.001\,min^{-1}$) albeit it showed a less favourable K_m ($11 \pm 1\,\mu M$) than the WT SsGBP recombinant protein. All other five mutants resulted in lower catalytic activity (Fig. 1B). In particular, N189P, T193N and G235P completely lost their GTP hydrolysis activities; the G235S mutation significantly decreased the activity (Fig. 1B); and T213V resulted in a >50% decrease in k_{cat} ($0.011 \pm 0.001\,min^{-1}$) compared to WT SsGBP (Fig. 3B). These kinetic data of the mutants were in line with our structural predictions extrapolated from previous Ras-like small GTPase data and suggested that, like those of classical small GTPases, P-loop, switches I and II of SsGBP are essential for its GTPase activity.

To further rule out a possibility that the observed loss of GTPase activity in some SsGBP variants was caused by defects in their protein folding and/or stability, we performed a thermofluor analysis on all recombinant proteins of SsGBP variants included in this study (Fig. 4). Thermofluor is a technique that uses the fluorescent signal from a non-specific ligand to monitor denaturation of a protein in response to temperature increase (*12*). The corresponding temperature at

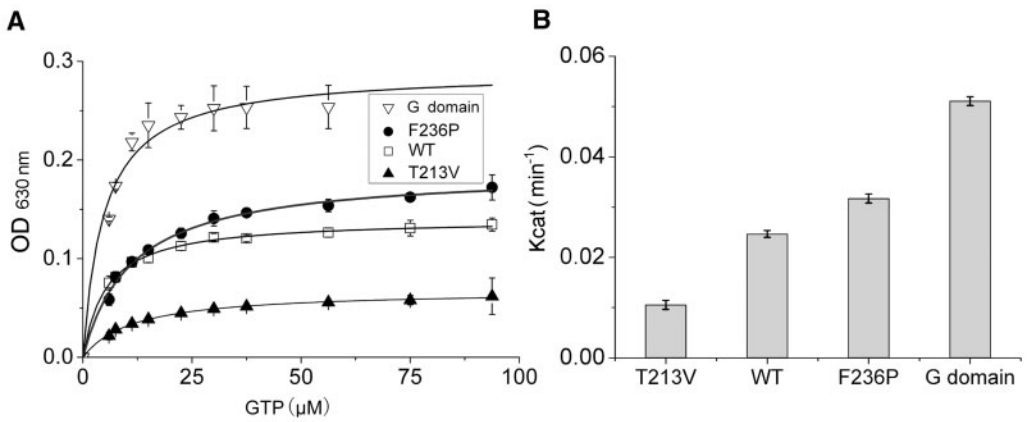

Fig. 3 Kinetics of GTP hydrolyses by the full-length WT SsGBP, G-domain and mutation variants T213V and F236P. (A) Michaelis–Menten plot showing variation of GTPase activity of different protein samples versus substrate concentration. For each reaction point, 1.7 μM protein (in the case of T213V, 5 μM protein was used to compensate its low activity in the experiment, and subsequently the OD values shown on this plot were the experimental data divided by 3.0) was incubated at 50°C for 100 min with the indicated concentration of GTP in a buffer of 20 mM Tris–HCl (pH 7.5), 150 mM NaCl and 5 mM $MgCl_2$ in a final volume of 100 μl. The reaction was terminated with 25 μl GOLD-mix. Each point represents the mean ± SD from three measurements. (B) Values of k_{cat} with 95% confidence interval of WT SsGBP, F236P, T213V and the G-domain.

which the slope of the fluorescent-temperature curve stop growing during the major denaturation of the protein sample is defined as the melting temperature (T_m). Consistent with its thermophilic origin, the full length WT SsGBP showed a T_m of 77°C in the absence of guanine nucleotide. N189P, T193N, T213V and G235S varied their T_m within 4°C around that of the full-length WT SsGBP, and G235P was the most stable variant in this study with a T_m of 83°C. In contrast, the isolated GTPase domain and F236P showed a significant loss in thermal stability with T_m of 48°C and 53°C, respectively, and their thermal denaturing curves were also broader than others (Fig. 4A and D). Similar conclusions held true for assays in the presence of GDP or GTP. Because of possible non-specific binding of nucleotide to SsGBP (*1*), we choose not to over-interpret differential data between thermofluor assays with and without GDP/GTP. Nevertheless, the general trend was that guanine nucleotide binding increases T_m. From available data, we concluded that the variation of GTPase activity among SsGBP variants does not positively correlate with their thermal stability changes, and the GTPase activity measurement of our recombinant proteins used in this study likely reflected their intrinsic GTP hydrolysis abilities.

Crystal structures of SsGBP variants G235P and G235S

To further investigate structure–function relationship of mutations at the conserved Gly235 in SsGBP, we performed crystallography studies on the G235P and G235S variants. Mutant G235P was crystallized under a similar condition to our WT SsGBP crystal form yet in the absence of GDP, NaF and $AlCl_3$. The G235P crystal form belongs, however, to a different space group, $P2_1$. Crystallography refinement resulted in a 2.3 Å resolution structure with $R_{work} = 0.25$ ($R_{free} = 0.27$). In this monoclinic crystal form, there are two protein molecules (A and B) per asymmetric unit, with a solvent content 49% and Matthews coefficient $V_M = 2.4$ Å^3/Da. Total 579 amino acid residues and 65 solvent molecules were included in the final refined model. The two protein molecules are related by a pseudo two-fold axis with a rotation angle 177° and a screw length 1.3 Å. The r.m.s.d. between G235P molecules A and B is 1.0 Å for 284 Cα pairs.

Mutant G235S was crystallized under a similar condition to G235P, and we determined its structure at 2.5 Å resolution with final $R_{work} = 0.24$ ($R_{free} = 0.26$). The G235S crystal form is essentially the same as that of G235P. Total 586 amino acid residues and 67 solvent molecules were included in the final refined model. Similar to the G235P crystal form, the r.m.s.d. between G235S molecules A and B was 1.0 Å for 290 Cα pairs. The overall crystal contents of the two mutant crystals were even more similar. For example, the r.m.s.d. between molecules A from the G235S and G235P crystal forms was 0.4 Å for 293 Cα pairs. In the following, we consider these two crystal forms are identical except at the mutation site.

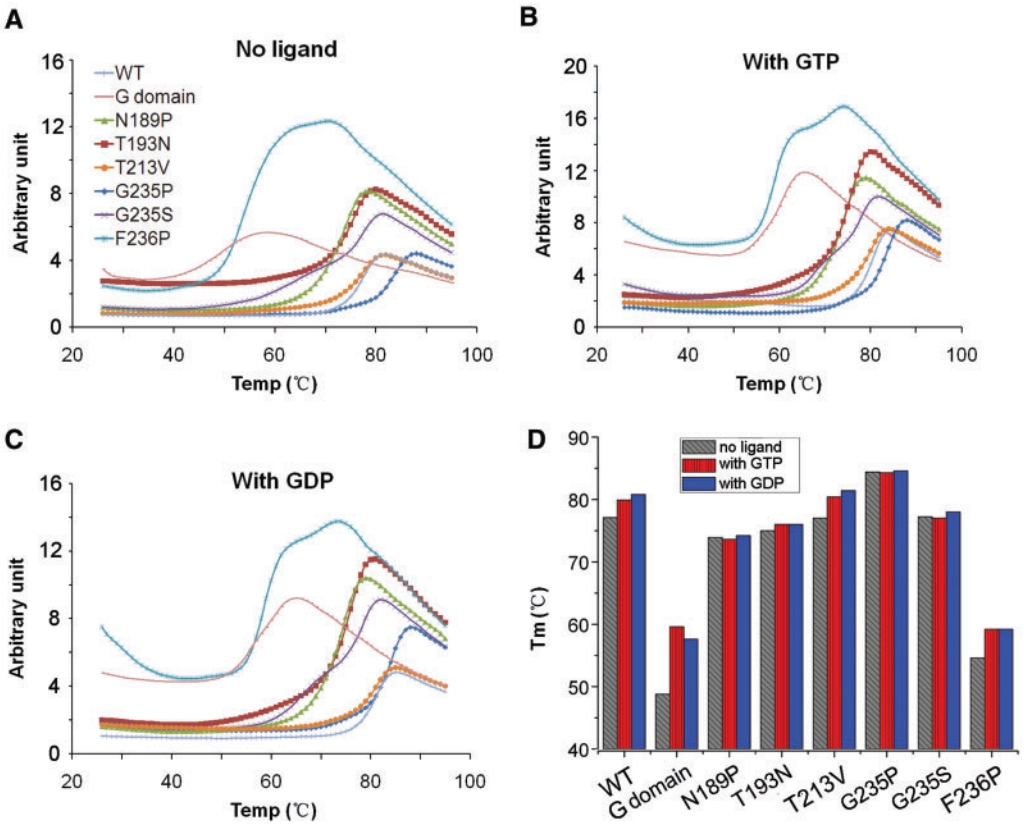

Fig. 4 Thermofluor analysis of WT SsGBP, six variants of point mutations and the isolated G domain. Raw data of every SsGBP variants in a buffer of 20 mM Tris–HCl (pH 7.5) and 150 mM NaCl in the absence of guanine nucleotide (A), the presence of GDP (B) or GTP (C) are shown. Deduced T_m values are shown in (D). The colour codes of panels (B) and (C) are the same as that of panel (A).

In order to investigate structural changes associated with mutation at position 235, the G235P structure was compared to that of WT SsGBP. Molecules A and B of G235P showed a 1.2 Å r.m.s.d. for 288 Cα pairs and 0.9 Å for 285 Cα pairs, respectively, with WT. In addition, we found that this single point mutation barely affected local structure around the active site (Fig. 2C). For instance, after overall superposition, the Cα r.m.s.d. between the P-loop (residue 186–193) and switch II (residue 232–256) of WT SsGBP and those of molecules A and B of G235P were 0.9 Å and 0.5 Å, respectively, smaller than the corresponding overall Cα r.m.s.d.; the same calculations for G235S gave 1.0 Å and 0.7 Å, respectively. Alternatively, the peptide φ-ϕ torsion angles between positions 234 and 235 were (137.2°, −74.0°) for WT and (130.6 ± 1.3°, −66.6 ± 0.5°) for G235P (where the values are the mean ± SD from molecules A and B). Nevertheless, there were clear but localized differences between structures of G235P and WT SsGBP somewhere away from the active site because of crystal packing changes. For example, residues 142–167 composed a long helix in WT SsGBP became mobile and difficult to trace in the G235P crystal structure. The hydrophobic surface covered by residues 142–167 in the WT SsGBP crystal form mediated an interaction between neighbouring protein molecules in the G235P crystal form. More important to the following discussion, the residue 235 was not involved in any crystal packing in our crystals of WT SsGBP•GDP, G235P and G235S. Therefore, we concluded that the structural effects of the point mutation at position 235 are localized only in the vicinity of the mutation site.

Discussion

Putative mechanism of GTP hydrolysis in SsGBP

SsGBP belongs to the HflX family (*1*, *2*), members of which share amino acid sequences and presumably 3D structural similarity in their C-terminal domains (G-domain) with the Ras related GTPases. In this work, we demonstrate that SsGBP also shares similar local structures and functions in its Mg^{2+}-binding site (Figs 1A and 2A) and P-loop (Figs 1B, 2B and 3) in addition to its overall structure with Ras-like small GTPases. However, unlike most small GTPases, HflX family members do not have the highly conserved DxxGQ motif (*e.g.* ^{57}DTAGQ^{61} in human Ras and ^{75}DTAGQ^{79} in Rab5) in the so called switch II region which changes conformation in response to guanine nucleotide binding or hydrolysis. The Gln residue in DxxGQ stabilizes the transition state during GTP hydrolysis by coordinating the nucleophilic water molecule to attack the γ phosphoryl group of GTP (*10*). In SsGBP, this Gln residue corresponds to position 236 and is replaced by a Phe residue (Fig 2B and Supplementary Fig. S2). In order for the GTP hydrolysis to occur in SsGBP, there must be some other group(s) performs the same function as what the glutamine side chain from the DxxGQ motif does. Such a group may come from either the N- or G-domain. Because an isolated G-domain has a higher intrinsic GTP hydrolysis activity than the full length SsGBP (Figs 1B and 3), the group that aligns a nucleophilic water molecule for attacking the γ-phosphoryl group is likely to be contributed by the G-domain. We hypothesized that this functional group is the main chain amide group of Gly235 from the ^{232}DTVGF^{236} sequence, because it is the only polar group from the G-domain, based on geometry inspection of WT SsGBP crystal structure, that could possibly align a nucleophilic water molecule for attacking the γ-phosphoryl group from the axial direction of the $O_{\beta\gamma}$–P_γ bond (Fig. 2B).

Although Gly235 of SsGBP is conserved in other small GTPases, it does not necessarily mean that this glycine residue assumes the same function in different proteins. In Ras, Gly60 resides at a hinge region connecting a β-strand (β3) and an α-helix (α2) and facilitates the switching of Gln61 from an inactive position to the active position for aligning the nucleophilic water molecule (*18*, *19*). In fact, the absolutely conserved Gly60 undergoes a huge change in backbone dihedral angles in response to the transformation from the ground state to transition state during GTP hydrolysis, and such a backbone change prefers a glycine residue for its flexibility (*18*, *19*). In SsGBP, Gly235 does not appear located in a hinge position equivalent to Gly60 in Ras (Fig. 2B). Additionally, the backbone flexibility associated with Gly235 is diminished in SsGBP because of the anchoring effect of Phe236 (see below). Therefore, we speculated that Gly235 assumes a function different from Gly60 in Ras, *e.g.* using its backbone amide group to align the nucleophilic water molecule. If this was true, mutating Gly235 to proline would prevent the main chain amide group from forming a hydrogen bond, resulting in a complete inhibition of GTP hydrolysis activity of G235P without necessarily altering the local structure of active site. Our mutagenesis data (Fig. 1B) support such a hypothesis. Furthermore, structural inspection showed that replacing Gly235 with proline did not affect the local structure of the active site (Fig. 2C) and would not disrupt GTP-binding. In addition, a similar mutation variant in Ras, G60A, does not affect GTP/GDP binding as shown in Ras–ligand complex structures of 1XCM and 1XJ0 from PDB. In order to further rule out a possibility that G235P simply did not bind GTP, we performed a MANT–GTP [2′ (3′)-O-(*N*-Methylanthraniloyl)-substituted GTP analogues]-binding assay which are frequently used for small GTPases (*20*, *21*). However, the signal was lost in a highly noisy background (data not shown) presumably due to non-specific nucleic-acid binding by SsGBP (*1*). Taken together, currently available data do not favor the possibility that the absence of GTPase activity in G235P was simply caused by stereo conflict between the proline side chain and the substrate GTP. Consistent with such a notion, the mutation variant of G235S which retained the backbone amide group showed significantly higher GTPase activity than G235P albeit lower than WT (Fig. 1B). In this case, the activity loss of G235S relative to WT could be explained by its side chain disruption of the nucleophilic water molecule. A counter argument could be that the backbone flexibility at position 235

is required for the activity. For instance, a serine residue is more flexible than proline but more rigid than glycine, and activities of point mutations at this position appear following the same trend. However, since the DxxGF sequence in SsGBP is anchored to the main body of the G-domain by Phe236, the flexibility of position 235 may be less critical than its potential to serve as a proton donor. Furthermore, in order to probe another residue in the HflX-specific DxxGF sequence, Phe236, whose position corresponds to the classical catalytic glutamine residue (*e.g.* Gln61 in Ras and Gln79 in Rab5), we constructed the F236P mutant of SsGBP. Instead of losing GTP hydrolysis activity, F236P showed a higher k_{cat} than WT SsGBP (Fig. 3), indicating that the main chain amide group of Phe236 is not required for aligning the nucleophilic water molecule. More details of this mutation are discussed later. Taken together, our current data are consistent with the notion that the nucleophilic water molecule for GTP hydrolysis in SsGBP is provided by the backbone amide group of Gly235 in the DxxGF sequence.

In addition to aligning the nucleophilic water molecule, the generally accepted mechanism of GTP hydrolysis in small GTPases includes another critical element: the P-loop offers a backbone amide group (*e.g.* Gly13 in Ras and Ala30 in Rab5, corresponding to Asn189 in SsGBP) to interact with the β−γ bridge oxygen ($O_{\beta\gamma}$) of GTP via a hydrogen bond. We speculated that this function of P-loop remains the same in SsGBP. Previously, it has been shown that mutation of equivalent Ala30 in Rab5 to proline abolishes the GTP hydrolysis activity without disturbing the overall structure (*7*, *15*). Similarly, the mutation of N189P in SsGBP results in a nearly total loss of the GTP hydrolysis activity (Fig. 1B). We also made the T193N mutant in SsGBP. It is located at the last position of P-loop motif but at the opposite side of the bound GDP/GTP from the P-loop (Fig. 2B). This mutation is similar to the classical 'SN' mutation which usually renders the protein to bind GDP only but not GTP by disturbing the magnesium site thus preventing the proper loading of substrate GTP (*16*). As a result, the classical 'SN' mutation will not hydrolyse GTP. The observation that T193N loses GTP hydrolysis activity (Fig. 1B) fits our expectation well. In addition, the corresponding S243N mutation of *C. pneumoniae* HflX caused a similar loss of GTP hydrolysis activity (*5*). This underlines that the P-loop in SsGBP and HflX GTPases in general retains its function(s) as in other classical GTPases.

Effects of SsGBP N-domain on GTP hydrolysis

Unlike Ras-like small GTPases, SsGBP and other HflX members are multi-domain proteins. In SsGBP, the N-domain (residue 1–178) interacts with the G-domain (residue 179–356) intra-molecularly through an extensive interface of about 2,000 $Å^2$ buried-solvent accessible surface contributed by both domains. Because the isolated GTPase domain processes a higher GTP hydrolysis activity than full length WT SsGBP, we speculated that N-domain binding is inhibitory to the GTP hydrolysis of G-domain. To investigate such a possibility, we made a point mutation, F236P, in the context of full length SsGBP. In both the SsGBP crystal structures with and without GDP, Phe236 anchors the switch II to a hydrophobic core of the GTPase domain (Fig. 2B) and allows switch II to have an extended conformation to interact with the N-domain (*1*). Thus, it is expected that mutating Phe236 to proline will alter the interaction of switch II with the hydrophobic core thus weakening the binding of N-domain to G-domain and increasing the GTP hydrolysis activity of SsGBP. Consistent with this prediction, we observed a decrease of thermal stability and a k_{cat} increase of GTP hydrolysis in the F236P mutant relative to the full length WT SsGBP (Figs 3, 4A and 4D). In addition, a proline residue brings more rigid to the peptide backbone than a phenylalanine residue could do, yet the corresponding mutant is less stable in our thermofluor assay (Fig. 4). It illustrates that local peptide rigidity is less effective to the N-domain binding than the overall stability of switch II achieved by the Phe236 anchoring.

One possible structural explanation for the inhibitory effect of the N-domain on GTPase activity is that the N-domain prevents switch I from binding GTP. Switch I is mobile in the SsGBP•GDP complex crystal structure, and such a mobility has been observed in many other GDP•small GTPase complexes (*3*). Upon binding GTP, this switch I region usually interacts with 'active site' Mg^{2+} ion via a chelate hydrogen bond. Thus, both the substrate and switch I become stabilized, and the switch I often becomes visible in crystal structures of GTP-complexes. By superimposing GTPase domain from our SsGBP•GDP structures with that of the Ras•GTP complex (PDB ID: 6Q21), we find that if switch I region of SsGBP was placed in a similar position as in Ras•GTP the former would collide with its own N-domain (Fig. 2D). In other words, the N-domain must disassociate from the G-domain in order for the switch I region to contact the bound GTP substrate unless switch I region in SsGBP did not work as it does in Ras, *i.e.* offering a chelate hydrogen bond to interact with the catalytic Mg^{2+}. To distinguish these two possibilities, we made the T213V mutant (Fig. 2B). Residing in switch I, Thr213 is absolutely conserved in the HflX family. It is the residue putatively offering its side chain to form a chelate hydrogen bond with the Mg^{2+} ion. T213V would eliminate the potential proton donor group for chelate hydrogen bonding with the Mg^{2+} while maintaining the geometry. Since the point mutation of T213V results in 50% decrease in k_{cat} (Fig. 3B), we believe that SsGBP switch I region, in particular Thr213, retains its function in GTP-binding and perhaps GTP hydrolysis as does the equivalent residue(s) in Ras. This is also confirmed by the strongly reduced GTP hydrolysis activity of the corresponding T263A mutant of *C. pneumoniae* HflX (*5*).

Active GTP-bound form and Inactive GDP-bound form of SsGBP

Small GTPases and heterotrimeric G proteins (Gαβγ) all function as molecular switches in biological

signalling by cycling their conformations between GTP-bound and GDP-bound forms. Small GTPases adopt so called active conformations which are able to interact with their downstream effectors when they bind GTP. After hydrolyzing GTP to GDP, they change to inactive forms and dissociate with their effectors. For heterotrimeric G protein, the Gα subunit interacts with the Gβγ complex when it is in a GDP-bound inactive form. Once activated by binding GTP, Gα dissociates with Gβγ, and this dissociation facilitates the binding with downstream effectors (*22*, *23*). Analogous to this process, SsGBP behaves more similar to the Gαβγ system than to small GTPases. First, the N-domain might function analogous to Gβγ and probably plays a role of guanine nucleotide dissociation inhibitor (GDI) (*24*). Furthermore, upon N-domain dissociation, the G-domain may bind GTP and interact with downstream effectors. The 'free' N-domain itself may also become available to interact with other downstream effectors as does the Gβγ complex. The N-domain dissociation may be triggered by upstream signals. A possible candidate of such a signal(s) may come from nucleotide binding (*1*, *6*).

Interestingly, the phenomenon that the catalytic Gln is substituted by a hydrophobic residue while maintaining the GTPase activity is not unique to the HflX family. It has also been observed in some other GTPase families such as Era, EngA, TrmE and Nogl (*25*). Collectively these proteins are termed as hydrophobic amino acid substituted for catalytic glutamine GTPases (HAS-GTPases) (*25*). Characteristically, all HAS-GTPases contain extra domains in addition to the G-domain. As in SsGBP, their substitutions of a hydrophobic residue for the catalytic Gln in the DxxGQ motif all result in anchoring of switch II region to a hydrophobic core of the G-domain (*25*). We anticipate that HAS-GTPases share more functional properties and that SsGBP likely becomes a good model system for studying GTP hydrolysis mechanisms as well as their regulations in HAS-GTPases because of its excellent properties such as the unusual thermal stability of recombinant SsGBP (Fig. 4).

To summarize, in this work we report data of a number of SsGBP point mutations from GTPase activity assays, thermofluor based stability analyses and X-ray crystallography analyses. Our results indicate that the conservation of a hydrophobic residue in HflX GTPases at the classical glutamine position is related to the stability of the C-terminal GTPase domain and to its interaction with the N-terminal HflX domain. A higher stability of the GTPase domain seems related to a tighter regulation of the intrinsic GTPase activity. Moreover, inspection of the SsGBP crystal structures suggests that the backbone amide group of Gly235 of the DxxGF sequence is the most likely choice of replacing the classical glutamine side chain in a Ras-like GTPase. Such a hypothesis is supported by our functional and structural analyses of G235P and G235S mutants in the DxxGF sequence of SsGBP.

Methods

Protein purification and mutagenesis

Constructs of WT SsGBP from *S. solfataricus* (GenBank ID 15897212) and its isolated G domain (*i.e.* residues 179–356) in the pET-24-d expression vector were described previously (*1*). Mutant variants of N189P, T193N, T213V, G235P, G235S and F236P were made from the WT SsGBP template with the Quick Change Mutagenesis kit (Agilent Technologies, Inc., La Jolla, CA, USA; Cat. #200518). All mutations were confirmed using full-length DNA sequencing. C-terminal His-tag fused recombinant proteins were overexpressed in the *E. coli* BL21 (DE3) strain at 37°C for 5 h after induced with isopropyl β-d-thiogalactopyranoside (IPTG) at a final concentration of 1.0 mM. For WT SsGBP expression, the cell lysate was heated at 65°C for 25 min to precipitate contaminating *E. coli* proteins, and the SsGBP protein was further purified with Ni-affinity chromatography and Superdex 200 (GE Healthcare) gel filtration following a previously described procedure (*13*). SsGBP mutant variants were purified in a similar way yet without applying the 65°C treatment. All samples of purified recombinant fusion proteins were used directly for subsequent studies without cleaving off the C-terminal His-tag.

Colorimetric assay of GTP hydrolysis

GTPase activities of WT SsGBP, G-domain, and every point mutation were measured by monitoring phosphate release during GTP hydrolysis using the malachite-green assay (*17*) in the absence of ribosome components. The Pi-ColorLock™ kit (Innova Biosciences, Cambridge, UK; Cat. #303-0125) was used for this assay following the manufacture instruction. In brief, Nunclon 96-well, flat bottom, white, polystyrol plates were used. GTP (100 μM) was incubated at 50°C with 5 μM SsGBP sample and 5 mM $MgCl_2$ (or $CaCl_2$ or $CdSO_4$) in a buffer of 20 mM Tris–HCl (pH 7.5) and 150 mM NaCl. Specified amount of sample (50 or 100 μl) was withdrawn at each predetermined time point. For each 100 μl reaction, 25 μl freshly prepared GOLD mix from the kit was added to terminate the reaction, and 10 μl stabilizer was added 5 min later. An Infinite-200 multimode reader (Tecan Group Ltd, Switzerland) was used to measure the $OD_{630\,nm}$ of each well. In order to estimates the amount of Pi-released from GTP-hydrolysis, a phosphate standard curve was made with triplicate measurements of each point following the manufacture instruction (data not shown).

The values of kinetic parameters of k_{cat} and k_m were determined by fitting the experimental data to the Michaelis–Menten equation by using Origin 7.5 (OriginLab Corporation, Northampthon, USA).

Thermofluor analysis

The thermofluor method (*12*) was used to measure and compare thermal stabilities of different SsGBP variants in the presence and absence of guanine nucleotide (*i.e.* GDP or GTP). The assay was performed in a 96-well, non-skirted, black lettered PCR plate

(Thermo Fisher Scientific, Cat. # AB-0600-L). Each well contained 0.1 mg/ml protein in a buffer of 20 mM Tris–HCl (pH 7.5), 150 mM NaCl and 5 × Sypro orange (Invitrogen/Molecular Probe, Eugene, OR, USA) as the fluorescent dye in a total volume of 20 µl. Should the corresponding ligand, GTP or GDP present, its final concentration was 5 mM with additional 5 mM $MgCl_2$. The plate was sealed with an Optical-Quality Sealing Tape (Bio-Rad, Hercules, CA, USA). Temperature scan was performed from 25 to 90°C with a scanning rate of +1°C per minute in a real-time PCR 7300 instrument (Applied Biosystem, Foster City, CA, USA). Fluorescence changes of each well were recorded during heating.

The temperature midpoint, so called melting temperature (T_m) was calculated by fitting the fluorescence data to a Boltzmann model according to a previous description (*12*),

$$I = \left(A + \frac{(B - A)}{1 + e^{(T_m - T)/C}} \right)$$

where I is the fluorescence intensity at temperature T, and T_m, A, B and C are constants to be determined. Data points after the maximum fluorescence intensity were excluded from the fitting.

Crystallization, structure determination

Crystals of WT SsGBP•GDP complex was grown using the hanging drop method at 16°C. The protein sample was stored at about 15 mg/ml concentration with 5 mM GDP in 20 mM Tris–HCl (pH 7.5), 150 mM NaCl, 5 mM $MgCl_2$, 80 mM NaF and 2 mM $AlCl_3$; and it was mixed 1 : 1 with the precipitant solution of 10% (w/v) polyethylene glycol (PEG) 3350 and 0.18 M sodium thiocyanate. Recombinant proteins of G235P and G235S variants were similarly crystallized but in the absence of GDP, NaF and $AlCl_3$.

Attempts of soaking ligand (5 mM GppNHp or GDP) into the G235P and G235S crystals for a time interval varied from several minutes to 3 days were made without success because of poor diffraction after soaking. Regarding co-crystallization, complex crystals of G235S with ligand (GppNHp or GDP) showed thin plate shapes and were unqualified for data collection. As for G235P, high diffraction quality crystals indeed appeared in the presence of ligands (GppNHp or GDP) after about 3 months, which was unusually long comparing with the 2 weeks of G235P crystallization in the absence of a ligand. However, ligands could not be identified from electron density maps either in the actives site or other surface positions of SsGBP from such G235P–ligand complex crystals, and the crystal form changed from space group $P2_1$ to P1 (data not shown).

After passing through the cryoprotection solution of 20% (v/v) glycerol, 10% (w/v) PEG 3350 and 0.18 M sodium thiocyanate, crystals of diffraction quality were plunged into 100 K cold nitrogen stream before data collection. Data sets of WT SsGBP•GDP, G235P and G235S were collected from an in-house Mar345 image-plate data collection system (Mar Research Inc., Norderstedt, Germany), an FR-E Bluemax X-ray data collection system (Rigaku, Japan), and the beamline 17A at the Photon Factory synchrotron facility (Tsukuba, Japan), respectively. The diffraction data were indexed, integrated, and scaled using the

Table I. Statistics of data collection and refinement.

	WT SsGBP•GDP	G235P	G235S
Data collection			
Space group	$P2_12_12_1$	$P2_1$	$P2_1$
Unit cell	$a = 67.3$, $b = 68.5$, $c = 92.1$	$a = 55.7$, $b = 71.2$, $c = 97.7$, $\beta = 96.8°$	$a = 55.6$, $b = 71.1$, $c = 97.1$, $\beta = 97.0°$
No. of unique Refls (Redundancy)	11,840 (2.7)	31,222 (4.0)	26,261 (3.9)
Resolution range(Å)	50.0 (2.74)[a]–2.65	50.0 (2.43) –2.35	50.0 (2.57) –2.50
I/σ(I)	14.2 (2.3)[a]	13.2 (2.5)	8.7 (3.8)
Completeness (%)	91.6 (87.9)[a]	98.4 (97.2)	99.8 (99.6)
R_{merge}[b](%)	7.9 (37.4)[a]	5.1 (40.8)	6.9 (36.4)
Refinement			
Resolution (Å)	23.23–2.65	38.82–2.35	38.37–2.50
[c]R_{free} (%)/$R_{working}$ (%)	29.0/22.4	26.6/24.4	26.4/24.0
Average B factor (Å^2)	60.7 (53.0)[d]	53.1 (44.3)	50.6 (41.7)
Protein	60.7	53.2	50.7
solvent	42.4	46.0	46.9
r.m.s.d. from ideal values			
Bond length (Å)	0.004	0.002	0.002
Bond angle (deg)	0.806	0.452	0.458
Ramachandran plot (%)[e]			
Favoured region	95.6	96.3	96.5
Allowed region	4.4	3.7	3.5
Outlier region	0.0	0.0	0.0

[a]Values in parentheses are for the highest resolution bin.
[b]$R_{merge} = \sum_{hkl} \sum_i I_i - < I > | / | < I > |$ where I_i is the intensity for the ith measurement of an equivalent reflection with indices h, k, l.
[c]$R = \sum |Fo - Fc| / \sum |Fo|$ where F_o and F_c are the observed and calculated structure factors, respectively.
[d]Values in parentheses is the Wilson B factor calculated using the program Truncate (*30*) in the CCP4 package (*31*) and data in the resolution range of 4.0 – 2.65 Å for WT SsGBP•GDP, 4.0 – 2.35 Å for G235P and 4.0 – 2.50 Å for G235S.
[e]Calculated using Procheck, version 1.00.0 (*32*).

program package HKL2000 (*26*). Phases of the three crystal structures were determined using the molecular replacement method implemented in the program Phaser (*27*) and a previously published SsGBP crystal structure [PDB ID 2QTF (*1*)] as the research model. Structures were built with Coot (*28*) and refined by using Phenix-refine (*29*) without applying NCS restrain for different molecules in the asymmetric unit of G235P and G235S. Solvent molecules were built conservatively, *i.e*. only those with good density and clear hydrogen bond interactions were accepted. Statistics of data collection and refinement are shown in Table I.

Coordinates of the final refined model and experimental structural factors have been deposited to the RCSB Protein Data Bank (http://www.rcsb.org/pdb/). The accession IDs are 3KXI for WT SsGBP•GDP complex, 3KXK for the G235P mutant and 3KXL for G235S.

Supplementary Data

Supplementary Data are available at *JB* Online.

Acknowledgements

The authors are grateful to Drs Guangpu Li and Simon Terzyan for helpful discussions. The authors also thank Ms Nancy Wakeham, Dr Weihong Li and staff members of the Structural Biology Core Facility in the Institute of Biophysics, Chinese Academy of Sciences (CAS), for their excellent technical assistance, especially to Mr Xudong Zhao, Mr Zhongnian Zhou, Mr Jianhui Li, Mr Yi Han and Ms Xiaoxia Yu.

Funding

The '863' Project (China) grant 2006AA02A322 to X.L. and grant 2006CB10903 (China) to X.C.Z.

Conflict of interest

None declared.

References

1. Wu, H., Sun, L., Blombach, F., Brouns, S.J., Snijders, A.P., Lorenzen, K., van den Heuvel, R.H., Heck, A.J., Fu, S., Li, X., Zhang, X.C., Rao, Z., and van der Oost, J. (2009) Structure of the ribosome associating GTPase HflX. *Proteins* **78**, 705–713
2. Leipe, D.D., Wolf, Y.I., Koonin, E.V., and Aravind, L. (2002) Classification and evolution of P-loop GTPases and related ATPases. *J. Mol. Biol.* **317**, 41–72
3. Vetter, I.R. and Wittinghofer, A. (2001) The guanine nucleotide-binding switch in three dimensions. *Science* **294**, 1299–1304
4. Jain, N., Dhimole, N., Khan, A.R., De, D., Tomar, S.K., Sajish, M., Dutta, D., Parrack, P., and Prakash, B. (2009) E. coli HflX interacts with 50S ribosomal subunits in presence of nucleotides. *Biochem. Biophys. Res. Commun.* **379**, 201–205
5. Polkinghorne, A., Ziegler, U., Gonzalez-Hernandez, Y., Pospischil, A., Timms, P., and Vaughan, L. (2008) Chlamydophila pneumoniae HflX belongs to an uncharacterized family of conserved GTPases and associates with the Escherichia coli 50S large ribosomal subunit. *Microbiology* **154**, 3537–3546
6. Shields, M.J., Fischer, J.J., and Wieden, H.J. (2009) Toward understanding the function of the universally conserved GTPase HflX from Escherichia coli: a kinetic approach. *Biochemistry* **48**, 10793–10802
7. Zhu, G., Liu, J., Terzyan, S., Zhai, P., Li, G., and Zhang, X.C. (2003) High resolution crystal structures of human Rab5a and five mutants with substitutions in the catalytically important phosphate-binding loop. *J. Biol. Chem.* **278**, 2452–2460
8. Jurnak, F., Heffron, S., and Bergmann, E. (1990) Conformational changes involved in the activation of ras p21: implications for related proteins. *Cell* **60**, 525–528
9. Der, C.J., Finkel, T., and Cooper, G.M. (1986) Biological and biochemical properties of human rasH genes mutated at codon 61. *Cell* **44**, 167–176
10. Pai, E.F., Krengel, U., Petsko, G.A., Goody, R.S., Kabsch, W., and Wittinghofer, A. (1990) Refined crystal structure of the triphosphate conformation of H-ras p21 at 1.35 A resolution: implications for the mechanism of GTP hydrolysis. *EMBO J.* **9**, 2351–2359
11. Barbieri, M.A., Li, G., Mayorga, L.S., and Stahl, P.D. (1996) Characterization of Rab5:Q79L-stimulated endosome fusion. *Arch. Biochem. Biophys.* **326**, 64–72
12. Ericsson, U.B., Hallberg, B.M., Detitta, G.T., Dekker, N., and Nordlund, P. (2006) Thermofluor-based high-throughput stability optimization of proteins for structural studies. *Anal. Biochem.* **357**, 289–298
13. Wu, H., Sun, L., Brouns, S.J., Fu, S., Akerboom, J., Li, X., and van der Oost, J. (2007) Purification, crystallization and preliminary crystallographic analysis of a GTP-binding protein from the hyperthermophilic archaeon Sulfolobus solfataricus. *Acta Crystallogr. Sect. F Struct. Biol. Cryst. Commun.* **63**, 239–241
14. Scheffzek, K., Ahmadian, M.R., Kabsch, W., Wiesmuller, L., Lautwein, A., Schmitz, F., and Wittinghofer, A. (1997) The Ras-RasGAP complex: structural basis for GTPase activation and its loss in oncogenic Ras mutants. *Science* **277**, 333–338
15. Li, G. and Liang, Z. (2001) Phosphate-binding loop and Rab GTPase function: mutations at Ser29 and Ala30 of Rab5 lead to loss-of-function as well as gain-of-function phenotype. *Biochem. J.* **355**, 681–689
16. Li, G., Barbieri, M.A., Colombo, M.I., and Stahl, P.D. (1994) Structural features of the GTP-binding defective Rab5 mutants required for their inhibitory activity on endocytosis. *J. Biol. Chem.* **269**, 14631–14635
17. Geladopoulos, T.P., Sotiroudis, T.G., and Evangelopoulos, A.E. (1991) A malachite green colorimetric assay for protein phosphatase activity. *Anal Biochem* **192**, 112–116
18. Chang, M.H., Chae, K.S., Han, D.M., and Jahng, K.Y. (2004) The GanB Galpha-protein negatively regulates asexual sporulation and plays a positive role in conidial germination in Aspergillus nidulans. *Genetics* **167**, 1305–1315
19. Ford, B., Hornak, V., Kleinman, H., and Nassar, N. (2006) Structure of a transient intermediate for GTP hydrolysis by ras. *Structure* **14**, 427–436
20. Brownbridge, G.G., Lowe, P.N., Moore, K.J., Skinner, R.H., and Webb, M.R. (1993) Interaction of GTPase activating proteins (GAPs) with p21ras measured by a novel fluorescence anisotropy method. Essential role of Arg-903 of GAP in activation of GTP hydrolysis on p21ras. *J. Biol. Chem.* **268**, 10914–10919
21. Gille, A. and Seifert, R. (2003) 2′(3′)-O-(N-methylanthraniloyl)-substituted GTP analogs: a novel class of potent competitive adenylyl cyclase inhibitors. *J. Biol. Chem.* **278**, 12672–12679
22. Tesmer, V.M., Kawano, T., Shankaranarayanan, A., Kozasa, T., and Tesmer, J.J. (2005) Snapshot of

activated G proteins at the membrane: the Galphaq-GRK2-Gbetagamma complex. *Science* **310**, 1686–1690
23. Sprang, S.R. (1997) G protein mechanisms: insights from structural analysis. *Annu. Rev. Biochem.* **66**, 639–678
24. Sasaki, T., Kikuchi, A., Araki, S., Hata, Y., Isomura, M., Kuroda, S., and Takai, Y. (1990) Purification and characterization from bovine brain cytosol of a protein that inhibits the dissociation of GDP from and the subsequent binding of GTP to smg p25A, a ras p21-like GTP-binding protein. *J. Biol. Chem.* **265**, 2333–2337
25. Mishra, R., Gara, S.K., Mishra, S., and Prakash, B. (2005) Analysis of GTPases carrying hydrophobic amino acid substitutions in lieu of the catalytic glutamine: implications for GTP hydrolysis. *Proteins* **59**, 332–338
26. Otwinowski, Z. and Minor, W. (1997) Processing of X-ray diffraction data collected in oscillation mode. *Methods Enzymol.* **276**, 307–326
27. McCoy, A.J., Grosse-Kunstleve, R.W., Adams, P.D., Winn, M.D., Storoni, L.C., and Read, R.J. (2007) Phaser crystallographic software. *J. Appl. Crystallogr.* **40**, 658–674
28. Emsley, P. and Cowtan, K. (2004) Coot: model-building tools for molecular graphics. *Acta Crystallogr. D Biol. Crystallogr.* **60**, 2126–2132
29. Adams, P.D., Grosse-Kunstleve, R.W., Hung, L.W., Ioerger, T.R., McCoy, A.J., Moriarty, N.W., Read, R.J., Sacchettini, J.C., Sauter, N.K., and Terwilliger, T.C. (2002) PHENIX: building new software for automated crystallographic structure determination. *Acta Crystallogr. D Biol. Crystallogr.* **58**, 1948–1954
30. French, G.S. and Wilson, K.S. (1978) Acta. *Cryst.* **A34**, 517
31. Bailey, S. (1994) The CCP4 suite: programs for protein crystallography. *Acta Crystallographica D* **50**, 760–763
32. Laskowski, R.A., MacArthur, M.W., Moss, D.S., and Thornton, J.M. (1993) PROCHECK: a program to check the stereochemical quality of protein structures. *J. Appl. Crystallogr.* **26**, 283–291